Eur. Phys. J. E **20**, 81–87 (2006)
DOI 10.1140/epje/i2006-10006-4

THE EUROPEAN PHYSICAL JOURNAL E

Extension of the resonant scattering technique to liquid crystals without resonant element

P. Fernandes[1], P. Barois[1,a], E. Grelet[1], F. Nallet[1], J.W. Goodby[2], M. Hird[3], and J.-S. Micha[4]

[1] Centre de Recherche Paul-Pascal-CNRS, Université Bordeaux 1, Avenue A. Schweitzer, 33600 Pessac, France
[2] Department of Chemistry, University of York, York YO10 5DD, UK
[3] Department of Chemistry, University of Hull, Hull, HU6 7RX, UK
[4] European Synchrotron Radiation Facility (ESRF), BP 220, 38043 Grenoble, France

Received 20 January 2006 /
Published online: 17 May 2006 –

Abstract. We report X-ray resonant scattering experiments performed on the prototype liquid-crystalline compound MHPOBC doped with a chemical probe containing a resonant atom (selenium). We determined directly for the first time the microscopic 3- and 4-layer structure of the ferrielectric subphases (SmC^*_{FI1} and SmC^*_{FI2}) present in MHPOBC. Despite the low fraction of the selenium probe, the resonant signal is strong enough to allow an unambiguous determination of the basic structure of the ferrielectric subphases. These experiments demonstrate that the resonant scattering technique can be extended to liquid crystalline materials without resonant element and may stimulate new studies. A *non-resonant* Bragg reflection was also found in the SmC^*_{FI1} phase in pure MHPOBC, consistent with the 3-layer distorted model, but never detected before.

PACS. 61.30.Eb Experimental determinations of smectic, nematic, cholesteric, and other structures – 61.10.Nz X-ray diffraction

1 Introduction

Resonant scattering of X-rays has been used since 1998 as a unique and powerful tool to overcome the problem of forbidden Bragg reflections in chiral smectic-C liquid crystals [1–4]. It is well known that crystal periodicities associated with uniform helical axes do not produce Bragg reflections in conventional crystallography. The reason is that there is no modulation of the electron density associated with the helical symmetry. Resonant scattering occurs when the energy of the X-ray beam matches the absorption edge of an element of the sample. In this condition, the response of the resonant electron is so much amplified that the anisotropy of its local environment is no longer negligible. In this case, the structure factor must be taken as a tensor, whereas it reduces to a scalar in conventional crystallography. As a result, resonant Bragg peaks are observed in place of forbidden reflections and the polarization state of the resonant Bragg peaks is governed by the anisotropy of the tensor structure factor [5,6].

These properties have been successfully used to study the complex chiral structures of the antiferroelectric smectic-C phases and related subphases. The fundamental periodicities of the so-called SmC^*_α and ferrielectric phases SmC^*_{FI1} and SmC^*_{FI2} have been elucidated [1]. Polarization analysis of the resonant Bragg peaks has shown that some of the structural models (so-called Ising models) had to be ruled out [2,7] whereas high-resolution experiments have allowed a fine determination of the complex structure of the SmC^*_{FI2} phase [3], consistent with optical studies [8,9]. The main features of the various phases are summarized in Figure 1.

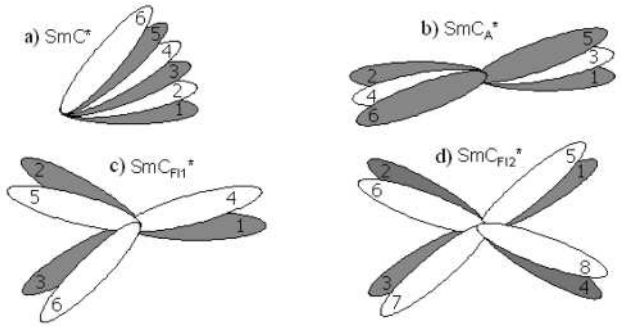

Fig. 1. Schematic representation of the projection of the director on the layer plane for various phases observed in chiral smectic-C systems: a) ferroelectric phase; b) antiferroelectric phase; c) ferri 1 phase; d) ferri 2 phase. The indices represent the layer position along the stacking axis.

[a] e-mail: barois@crpp-bordeaux.cnrs.fr

From a technical point of view, only a limited number of resonant elements can be used to conduct resonant scattering on liquid-crystal molecules. The absorption edges of light elements such as carbon or oxygen are too low in energy, whereas heavier elements may not be commonly found in liquid crystals. Practically, good candidates are elements of the third line of the periodic table heavier than silicon (*i.e.* phosphorus, sulfur and chlorine) and all elements of the fourth line (*i.e.* metals, arsenic, selenium and bromine). Phosphorus and arsenic, as trivalent elements, are not common in thermotropic liquid crystals, but resonance of phosphorus may be useful for structural studies of biological systems. Metals may be convenient for structural studies of metallomesogens. For all other liquid-crystalline materials (*i.e.* most synthetic liquid crystals designed for applications) four elements only are thus available for resonant scattering studies, namely sulfur, selenium, chlorine and bromine. All of them have been successfully used in resonant scattering studies. Resonance at sulfur and chlorine K-edges occurs at low energy (2.47 and 2.82 keV, respectively) hence requiring a specific beamline geometry to minimize X-ray absorption (freely suspended samples under a vacuum or helium flow [1,2]). Working at higher energies with selenium (12.66 keV) or bromine (13.47 keV) enables air flight paths and device geometries for electric field studies [10]. Experiments in this range have shown that the resonant signal is strong at selenium K-edge [11] whereas it is very weak with bromine for some reason unclear to us [12].

Most liquid crystals of interest however do not possess any of these four elements, preventing direct characterization of their structure. The aim of this paper is to show that X-ray resonant scattering studies can be carried out anyway in such materials by mixing a small amount of a liquid-crystal molecule possessing a resonant element with the material of interest. The foreign molecule acts as a probe, which reflects the microscopic structure of the host molecule. The observation of resonant scattering in the SmC^*_A phase of binary mixtures of liquid crystals containing various concentrations of resonant material (50, 25 and 10%) has been first reported in reference [4]. The present study explores the various subphases in the limit of lower concentrations, *i.e.* small enough to preserve the structure of the pure host material, but large enough to produce a useful resonant signal.

2 The materials

The prototype MHPOBC (4-(1-methylheptyloxycarbonyl) phenyl-4′-octyloxybiphenyl-4-carboxylate) compound was chosen as the host liquid crystal. MHPOBC is one of the most extensively studied materials exhibiting the antiferroelectric smectic-C phase and the related subphases [13]. The chemical formula and the phase sequence are given in Figure 2 as taken from reference [14]. Since the MHPOBC molecule does not possess any resonant element, it has never been studied by resonant scattering, which means that the microscopic structure of the subphases has never been characterized directly.

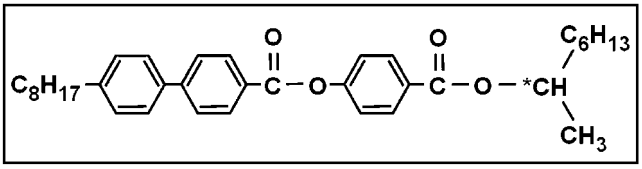

K • 84.0°C • SmC_A* • 118.4 • SmC_γ* • 119.2 • SmC* • 120.9 • SmC_α* • 122.0 • SmA • 148.0 • Iso

Fig. 2. Structure and phase sequence of MHPOBC taken from reference [14]. The S-enantiomer was used. Temperatures are in degrees Celsius.

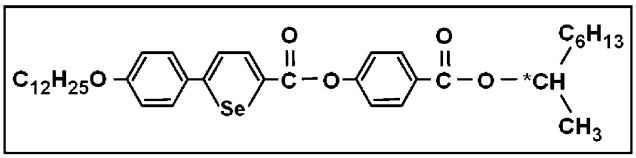

K • 67.7°C • SmC_A* • 97.8 • SmC_{FI1}* • 99.0 • SmC* • 109.4 • SmA • 116.6 • Iso

Fig. 3. Structure and phase sequence of PB237 (AS620) from reference [16]. The S-enantiomer was used.

The S-enantiomer of MHPOBC was purchased from Merck and used without any further purification. Differential scanning calorimetry scans performed on a Perkin-Elmer DSC 7 calorimeter on that commercial material revealed four phase transitions between the SmA and SmC^*_A phases. The observed phase sequence is then (heating runs, 0.2 °C/min):

$$SmC^*_A\text{-}(118.2\,^\circ C)\text{-}SmC^*_\gamma\text{-}(119.2)\text{-}SmC^*_\beta\text{-}(120.7)\text{-}SmC^*_\alpha\text{-}(122.0)\text{-}SmA.$$

As reported in previous studies ([13,15] and references therein), the identification of the SmC^*_γ and SmC^*_β phases is not always clear and may depend on the optical purity of MHPOBC. Following reference [15], SmC^*_γ and SmC^*_β correspond, respectively, to the SmC^*_{FI1} and SmC^*_{FI2} phases at high optical purity, and to the SmC^*_{FI1} and standard SmC^* phases at lower optical purity. At intermediate optical purity, all possible subphases may be present and the SmC^*_γ region may cover the two ferri structures SmC^*_{FI1} and SmC^*_{FI2}. We keep the notations with the γ and β subscripts to emphasize the uncertainty. Finally, one must keep in mind that the phase sequence may be affected by the free-standing film geometry.

The selenophene liquid crystal PB237 (referred to as AS620 in Ref. [16]) with molecular formula and phase sequence shown in Figure 3, was used as a probe. Its molecular architecture is close to MHPOBC, which certainly favors good mixing. The S-enantiomer was used in the mixtures. The choice of selenium as the resonant element enables simple diffraction conditions at 12.66 keV, available on most synchrotrons.

As always, the first thing to study with binary mixtures of liquid crystals is the phase diagram. Since the aim of the work is to study the structure of MHPOBC, it is interesting to investigate mixtures with a small amount of probe. Three mixtures were prepared with molar fractions

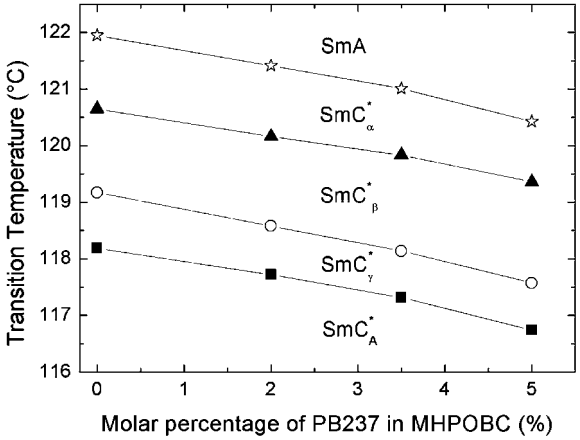

Fig. 4. Temperature shifts of the phase boundaries with increasing fraction of PB237 as detected by DSC scans upon heating.

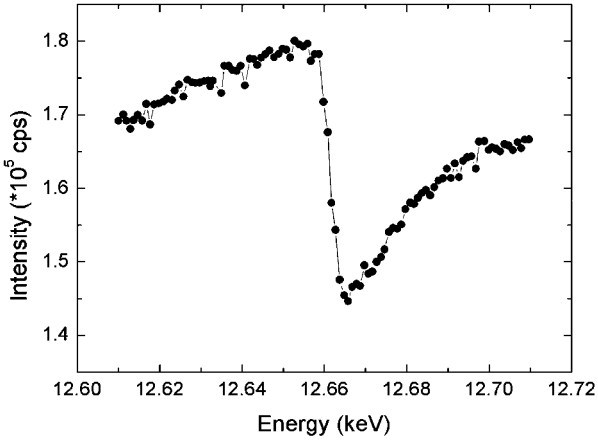

Fig. 5. Absorption scan of the selenium probe (PB237 K-edge = 12.661 keV).

of 2, 3.5 and 5%. To ensure sample homogeneity, after mixing the two products with the correct weight fractions, the mixture was dissolved in dichloromethane that was subsequently evaporated (by controlling both temperature and pressure).

The phase transitions were detected by DSC. The results presented in Figure 4 show that all the transition temperatures present a small and regular negative shift essentially proportional to the percentage of probe with a uniform slope of about $-0.30 \pm 0.02\,^{\circ}\mathrm{C}$ per % PB237 in the range $[0, 5\%]$. The number of phases in the mixtures remains unchanged.

3 X-ray experiments

The resonant X-ray scattering experiments were performed at beamline BM32 of the European Synchrotron Radiation Facility (ESRF) in Grenoble, using a three-circle diffractometer. The X-ray beam size was set to $50\,\mu$m (vertical) $\times\, 300\,\mu$m (horizontal) at sample position and the diffracted signal was collected by an NaI scintillator mounted on the two-theta arm. The in-plane (vertical) resolution estimated to $5{\cdot}10^{-4}$ Å^{-1} from the geometry was consistent with the $4.6 \cdot 10^{-4}$ Å^{-1} width of the resolution-limited (100) Bragg peaks.

The liquid-crystal samples were prepared as free-standing films drawn in the SmA phase to a size of 5 mm in width by 25 mm in length with typical thicknesses of about one micrometer. The samples were mounted in a two-stage oven (10 mK resolution) flushed with helium to minimize sample chemical degradation at high temperature, as well as scattering by air. In this geometry, the alignment of the smectic layers was better than 0.01 degrees as determined by transverse theta scans.

The resonant energy E_0 was first determined by an absorption scan through the PB237 pure material (Fig. 5). The energy of the beam was then set to $E_0 = 12.661$ keV.

The three different mixtures were then studied. All X-ray scans were recorded in the reflectivity geometry.

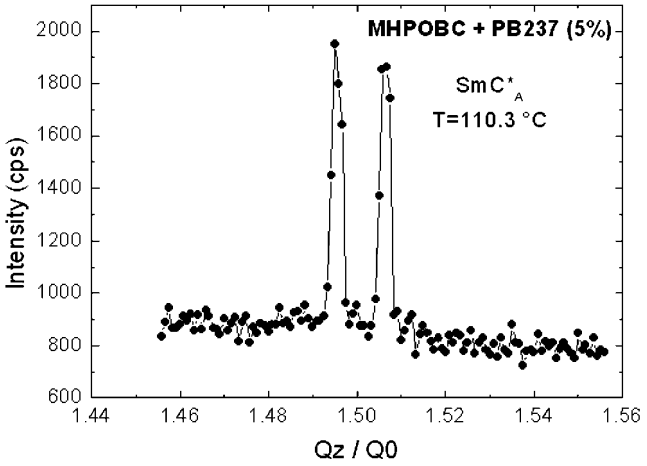

Fig. 6. 3/2 order resonant doublet in MHPOBC + PB237 (5%), $\mathrm{SmC}^*_{\mathrm{A}}$ phase at $T = 110.3\,^{\circ}$C. The splitting corresponds to a helical pitch of ~ 91 layers. The layer thickness deduced from the position of the (100) Bragg peak is 34.5 Å.

The quality and the alignment of each film were controlled by scanning the first (100) Bragg peak taken as a reference reciprocal vector $Q_0 = 2\pi/d$. The layer thickness d of the MHPOBC-PB237 smectic samples was in the range 33 to 37 Å depending on temperature and sample composition. The resonant signal was recorded at normalized wave numbers $H = Q/Q_0$ larger than 1 to avoid the strong non-resonant Fresnel background of the reflectivity signal.

The $\mathrm{SmC}^*_{\mathrm{A}}$ phase was investigated first. Figure 6 presents the resonant signal detected in the $H = 3/2$ region for the 5% mixture. A strong doublet centered on the 3/2 position is observed, characteristic of the 2-layer super-lattice of the $\mathrm{SmC}^*_{\mathrm{A}}$ phase. The splitting of the doublet indicates a helical pitch of 91 smectic layers ($\sim 0.3\,\mu$m). The width of the two resonant peaks is $4.5{\cdot}10^{-4}$ Å^{-1} FWHM, equal to the width of the resolution-limited (100) Bragg peak. Note that despite the low molar fraction of the probe, the signal is strong enough to allow

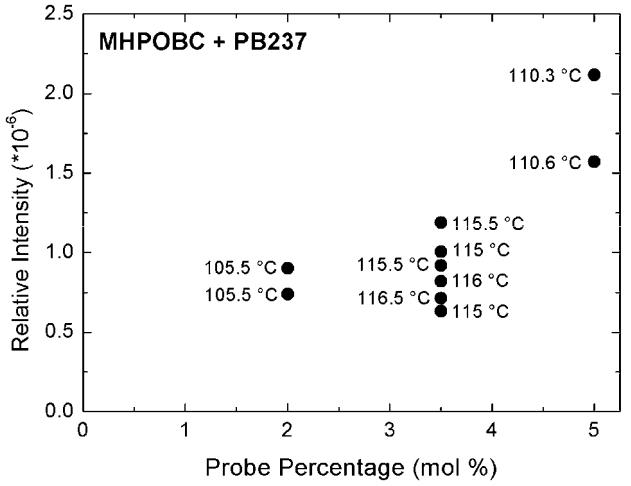

Fig. 7. Relative intensity of the resonant signal *versus* selenium probe percentage. Values are recorded on the 3/2 doublet of the SmC^*_A phase and are normalized by the intensity of the (100) peaks. Sets of data points correspond to different temperatures (as indicated) and different samples.

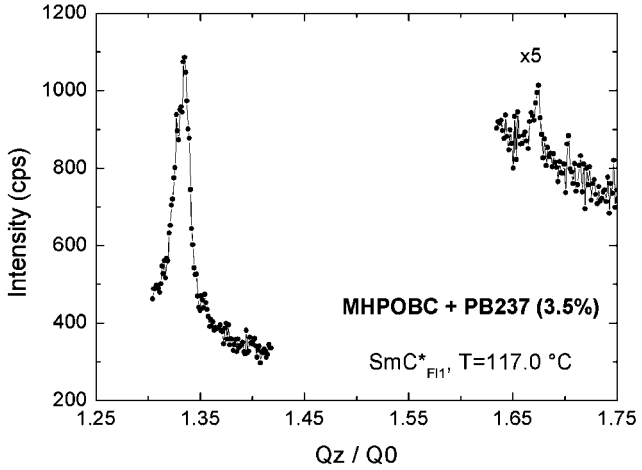

Fig. 8. 4/3 and 5/3 order peaks in MHPOBC + PB237 (3.5%), SmC^*_{FI1} phase, $T = 117.0\,^\circ$C.

good detection of sharp resolution-limited resonant peaks (counting time is 1 second per point).

Other mixtures have then been investigated in order to determine the dependence of the resonant signal on the percentage of selenium probe. Figure 7 shows a plot of the intensity of the resonant doublet in the SmC^*_A phase normalized by the intensity of the (100) peak for each film. Not surprisingly, the resonant signal increases monotonically with increasing fraction of PB237. The amount of probe can be reduced to less than 5%, hence minimizing its influence on the liquid crystal to study.

The SmC^*_γ region was then investigated at higher temperature for the three mixtures. In all cases, the 3/2 order doublet disappeared upon heating and the 4/3 and 5/3 order peaks characteristic of the 3-layer super-lattice of the SmC^*_{FI1} phase were observed. Figure 8 shows data recorded on the 3.5% mixture. The intense 4/3 order peak

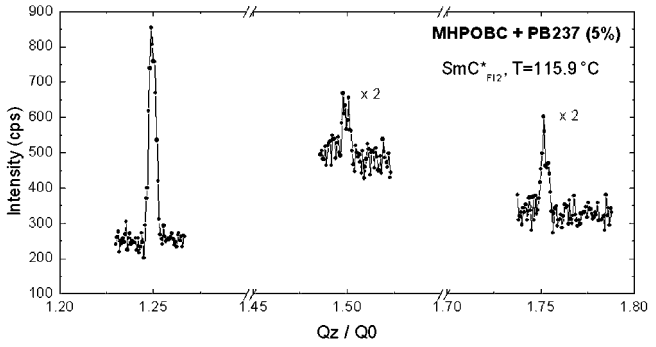

Fig. 9. Set of quarter order peaks (5/4, 6/4 and 7/4) observed in the SmC^*_{FI2} phase of the MHPOBC + PB237 (5%) mixture, $T = 115.9\,^\circ$C.

is about 5 times broader ($2.7 \cdot 10^{-3}$ Å^{-1} FWHM) than the instrumental resolution. A finer structure of the peak may exist that could not be resolved. The 5/3 order peak is much weaker but easily detectable. The same general features were observed on the 2% and 5% mixtures with no qualitative difference.

The 4/3 and 5/3 order peaks disappear upon further heating and the 5/4, 6/4 and 7/4 order peaks characteristic of the 4-layer super-lattice of the SmC^*_{FI2} phase are observed. This is shown in Figure 9 for the 5% mixture. The width of the most intense 5/4 and 7/4 peaks is $7.4 \cdot 10^{-4}$ Å^{-1} FWHM, 1.6 times larger than the instrumental resolution which suggests a distorted clock structure [3]. A finer characterization requires further studies for a more careful analysis of the lineshape. The splitting of the harmonic peak in 3/2 position ($\Delta Q = 5.5{\cdot}10^{-4}$ Å^{-1}) reveals a long pitch helix of about 320 layers ($\sim 1\,\mu$m). Once again, no qualitative difference was found between the three different mixtures.

The temperature was then raised to reach the SmC^* or SmC^*_α region. The quarter order resonant satellite disappeared above some temperature (depending on the mixture percentage), indicating the disappearance of the SmC^*_{FI2} phase, but despite careful studies on cooling and heating runs on several samples throughout the whole Q range, no resonant signal was detected above the SmC^*_{FI2} phase in any of the three mixtures. The analysis of the variation of the layer thickness *vs.* temperature (data not shown) clearly indicates though that there exists in all mixtures a tilted phase in the film in between SmC^*_{FI2} and SmA. The structure of this phase is just not detected.

The resonant nature of the non-integer Bragg peaks reported in three phases above can be easily checked by shifting the energy of the X-ray radiation. Figures 10 and 11 show the expected extinctions of the 3/2 and 5/4 peaks in the SmC^*_A and SmC^*_{FI2} phases, respectively. Note that an energy shift as low as 10 eV (less than 0.1%) is enough to kill the resonant signal.

Off-resonance scans of the non-integer Bragg peaks in the SmC^*_{FI1} phase gave a surprising result: unlike observed in other phases and reported in other experiments [1,2] the 4/3 order peak remained essentially unchanged upon shifting the energy by 20 eV (Fig. 12) or even 40 eV.

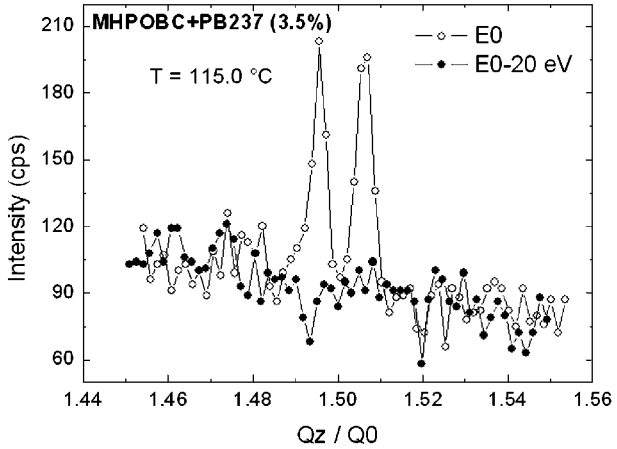

Fig. 10. Check of the resonant nature of the 3/2 Bragg peak in the SmC^*_A phase of the mixture MHPOBC + PB237 (3.5%), $T = 115.0\,^\circ$C.

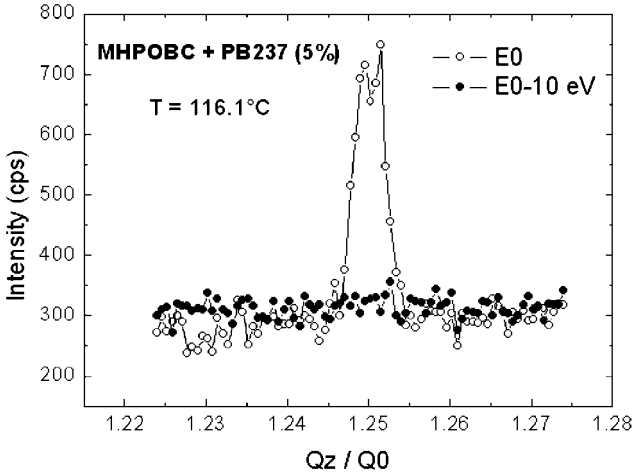

Fig. 11. Check of the resonant nature of the 5/4 Bragg peak in the SmC^*_{FI2} phase of the mixture MHPOBC + PB237 (5%), $T = 116.1\,^\circ$C.

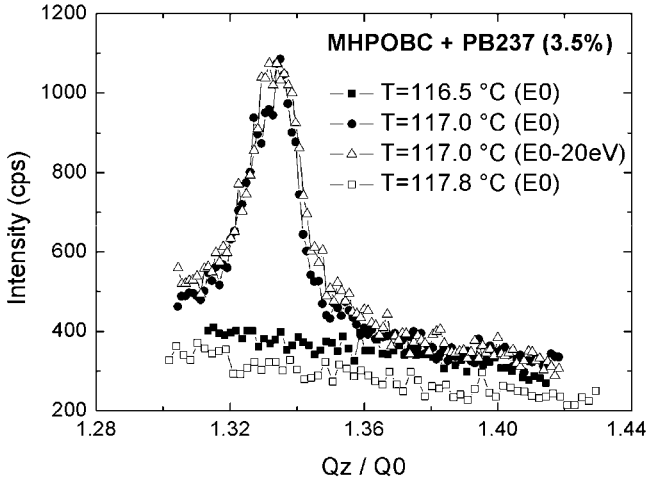

Fig. 12. Plots of the *non-resonant* 4/3 order Bragg peak in the SmC^*_{FI1} phase of the MHPOBC + PB237 (3.5%) mixture. The peak at $T = 117.0\,^\circ$C is not affected by a change in energy. It disappears at $T = 116.5\,^\circ$C in the SmC^*_A phase and at $117.8\,^\circ$C in the SmC^*_{FI2} phase.

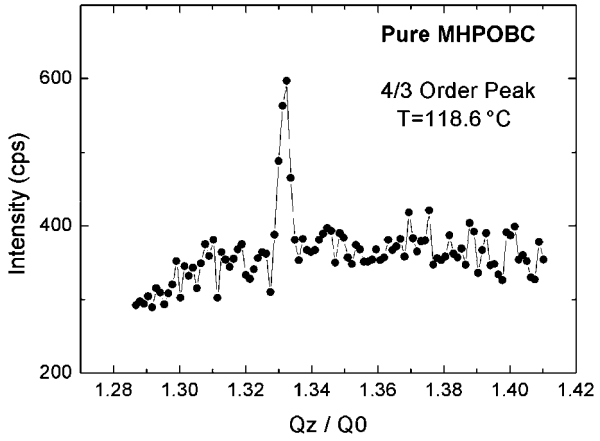

Fig. 13. Observation of a *non-resonant* 4/3 order Bragg peak in pure MHPOBC in the SmC^*_{FI1} phase, $T = 118.6\,^\circ$C.

Furthermore, Figure 12 shows that the 4/3 peak is temperature dependent and characteristic of the SmC^*_{FI1} phase: it disappears above and below the SmC^*_{FI1} phase, hence excluding the third-order harmonic of the X-ray beam as a possible cause of its appearance. We therefore conclude that the 4/3 peak of the SmC^*_{FI1} phase is non-resonant.

In order to check if the non-resonant Bragg peak was due to the presence of the selenophene probe, the same experiments were performed on pure MHPOBC. Figure 13 shows that the 4/3 order peak characteristic of the SmC^*_{FI1} phase is indeed present and sharp ($5.4 \cdot 10^{-4}$ Å^{-1} FWHM) in the pure material. To our knowledge, this is the first observation of a three-layer electron density modulation in MHPOBC and more generally in a SmC^*_{FI1} phase.

4 Discussion

The present work shows that molar fractions of a selenophene probe as low as a few percent (5, 3.5 and 2) produce a reasonably strong resonant signal. We reveal for the first time directly the 3-layer and 4-layer superlattice periodicities in the SmC_{FI} phases of MHPOBC.

Rigorously speaking, the structural data are collected in the mixtures and not in pure MHPOBC. Their validity in the limit of a pure material is questionable: it has been shown that low amounts of impurities (optical purity of MHPOBC [15] or a low percentage of foreign molecules [17]) can change the nature of the subphases or shift significantly their boundaries. The DSC data presented in Figure 4 show a simple shift of the phase boundaries towards lower temperatures with increasing fraction of selenophene material. This effect is standard in thermotropic liquid crystals. The regular shift of all the phase boundaries gives no evidence of any impurity-induced new phase transition. It is natural to believe that the phase sequence characterized in the mixtures is similar to the phase sequence of the pure host material. We therefore conclude that two SmC^*_{FI} phases exist in free-standing films of pure MHPOBC with a 3-layer and a 4-layer superlattice structure.

The absence of resonant signal in the SmC^* and/or SmC^*_α region may be due to experimental limitations and deserves further comments.

An insufficient instrumental resolution cannot explain the non-observation of the two pairs of resonant satellites in a SmC^* phase of too large helical pitch. In principle, the present X-ray setup enables detection of helical pitches as high as $0.6\,\mu$m [18]. Reported pitch values are below this limit [19] but not far below. Consequently, weak resonant SmC^* satellites may well be buried in the tails of the non-resonant peaks.

The situation is *a priori* more favorable in the SmC^*_α phase. The resonant peaks are usually more intense than in the SmC^* phase and they show up further away from the non-resonant Bragg peaks, *i.e.* on a lower background. In other words, the absence of detection of any resonant peaks is more difficult to explain in SmC^*_α than in SmC^* which suggests that the SmC^*_α phase did not show up in our films.

In summary, the arguments developed above suggest that our observations are consistent with the following phase sequence in free-standing films: SmC^*_A-SmC^*_{FI1}-SmC^*_{FI2}-SmC^*-SmA. The arguments in favor of the SmC* phase are weak however and we believe that this particular problem deserves further studies. The signal-to-background ratio could be improved in two ways: i) by collecting data over longer counting times and ii) by using a polarization sensitive detection system (which was not available in this experiment) in order to distinguish the π-polarized resonant satellite peaks from the σ-polarized background [2].

The non-resonant nature of the 4/3 peak was a surprise since all previously observed 4/3 peaks were resonant. Actually, the true surprise should be the fact that this non-resonant Bragg peak has not been detected before since it is simply allowed in the so-called distorted 3-layer model shown in Figure 1c. The forbidden reflection rule applies indeed for a 3_1 screw axis only, *i.e.* a uniform rotation angle of $2\pi/3$ between adjacent layers. The existence of this peak in pure MHPOBC shows that the corresponding 3-layer modulation of the electron density is not linked to the presence of the probe. We note however that the width of the 4/3 peak is larger in the mixtures, which suggests that the presence of the foreign molecule does not help the long-range ordering of the 3-layer structure. One may wonder why this non-resonant peak has not been observed before on the so much studied MHPOBC liquid crystal. The answer may be in its intensity which we find to be $2 \cdot 10^5$ lower than the main (100) Bragg peak. The combination of the strong ESRF synchrotron radiation with the excellent alignment of the free-standing film geometry is undoubtedly required to detect this weak peak

Finally, we must recall that a similar argument of symmetry applies to the distorted 4-layer phase for which the half-order reflections $Q_0/Q = \ell + 1/2$ are not forbidden [7]. These non-resonant half-order peaks were not detected in our experiments.

Experiments were also performed at the bromine K-edge with two other probes presented in Figure 14. Unlike the PB237 material, these bromine-substituted rod-like molecules are commercial, hence offering interesting possibilities for a wider extension of the technique. Despite the strong difference in molecular architecture, a good mixing with MHPOBC was achieved at the same set of concentrations (2 to 5%). The same phase sequence was observed, although with larger temperature shifts (the shifts were about 5 times larger than those observed on mixtures with PB237). Unfortunately, no resonant peaks were observed in any phases. This is consistent with previous experiments [12] and may indicate that the atomic anisotropy of polarization of bromine is too weak to produce a significant resonant signal.

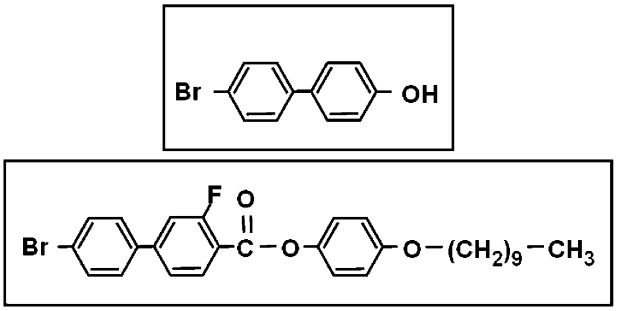

Fig. 14. Bromine probes molecular formulas (K-edge = 13.48 keV).

5 Conclusions

The method of mixing a resonant chiral probe with a non-resonant chiral liquid crystal, in order to determine the structure of the subphases appearing in the antiferroelectric chiral smectic-C systems has been successful. In the limit of low probe concentrations (2 to 5%), the resonant signal is strong enough to allow good determination of the fine structure of the subtle ferrielectric phases.

These experiments demonstrate that the resonant scattering technique can be extended to materials that possess no resonant atom. Selenium appears to be an excellent resonant element for the probe, since it produces a strong signal at a convenient energy. Experiments at bromine K-edge have been repeatedly disappointing. Foreign molecules with a sulfur element may be another option at lower energy.

This technique was applied to the well-known MHPOBC liquid crystal. We determined directly and for the first time the microscopic super-lattice structure of the ferrielectric subphases (3-layer SmC^*_{FI1} and 4-layer SmC^*_{FI2}) present in MHPOBC.

A non-resonant Bragg reflection was found in the SmC^*_{FI1} phase of the mixtures and of the pure MHPOBC material, consistent with the 3-layer distorted model, but never detected before.

The authors wish to thank Suntao Wang, Zenggiang Liu, B. McCoy, R. Pindak and H. Gleeson for helpful discussions. P. Fernandes thanks the Portuguese Foundation for Science and Technology (FCT) for financial support.

References

1. P. Mach, R. Pindak, A.-M. Levelut, P. Barois, H.T. Nguyen, C.C. Huang, L. Furenlid, Phys. Rev. Lett. **81**, 1015 (1998).
2. P. Mach, R. Pindak, A.-M. Levelut, P. Barois, H.T. Nguyen, H. Baltes, M. Hird, K. Toyne, A. Seed, J.W. Goodby, C.C. Huang, L. Furenlid, Phys. Rev. E **60**, 6793 (1999).
3. A. Cady, J.A. Pitney, R. Pindak, L.S. Matkin, S.J. Watson, H.F. Gleeson, P. Cluzeau, P. Barois, A.-M. Levelut, W. Caliebe, J.W. Goodby, M. Hird, C.C. Huang, Phys. Rev. E **64**, 050702(R) (2001).
4. L. Hirst, S.J. Watson, H.F. Gleeson, P. Cluzeau, P. Barois, R. Pindak, J. Pitney, A. Cady, P.M. Johnson, C.C. Huang, A.-M. Levelut, G. Srajer, J. Pollmann, W. Caliebe, A. Seed, M.R. Herbert, J.W. Goodby, M. Hird, Phys. Rev. E **65**, 041705 (2002).
5. D.H. Templeton, L.K. Templeton, Acta Crystallogr., Sect. A **42**, 478 (1986).
6. V.E. Dmitrienko, Acta Crystallogr., Sect. A **39**, 29 (1983).
7. A.-M. Levelut, B. Pansu, Phys. Rev. E **60**, 6803 (1999).
8. T. Matsumoto, A. Fukuda, M. Johno, Y. Motoyama, T. Yui, S. Seomun, M. Yamashita, J. Mater. Chem. **9**, 2051 (1999).
9. P.M. Johnson, D.A. Olson, S. Pankratz, T. Nguyen, J. Goodby, M. Hird, C.C. Huang, Phys. Rev. Lett. **84**, 4870 (2000).
10. L.S. Matkin, H.F. Gleeson, P. Mach, C.C. Huang, R. Pindak, G. Srajer, J. Pollmann, J.W. Goodby, M. Hird, A. Seed, Appl. Phys. Lett. **76**, 1863 (2000).
11. L.S. Matkin, S.J. Watson, H.F. Gleeson, R. Pindak, J. Pitney, P.M. Johnson, C.C. Huang, P. Barois, A.-M. Levelut, G. Srajer, J. Pollmann, J.W. Goodby, M. Hird, Phys. Rev. E **64**, 021705 (2001).
12. Although measurable, the resonant signal obtained with bromine was very weak. P. Cluzeau, P. Gisse, V. Ravaine, A.-M. Levelut, P. Barois, C.C. Huang, F. Rieutord, H.T. Nguyen, Ferroelectrics **244**, 301 (2000).
13. A.D.L. Chandani, E. Gorecka, Y. Ouchi, H. Takezoe, A. Fukuda, Jpn. J. Appl. Phys. **28**, L1265 (1989); E. Gorecka, A.D.L. Chandani, Y. Ouchi, H. Takezoe, A. Fukuda, Jpn. J. Appl. Phys. **29**, 131 (1990).
14. K. Hiraoka, A. Taguchi, Y. Ouchi, H. Takezoe, A. Fukuda, Jpn. J. Appl. Phys., Part 2, **29**, L103 (1990).
15. E. Gorecka, D. Pociecha, M. Čepič, B. Žekš, R. Dabrowski, Phys. Rev. E **65**, 061703 (2002).
16. J.T. Mills, H.F. Gleeson, J.W. Goodby, M. Hird, A. Seed, P. Styring, J. Mater. Chem. **8**, 2385 (1998).
17. N.W. Roberts, S. Jaradat, L.S. Hirst, M.S. Thurlow, Y. Wang, S.T. Wang, Z.Q. Liu, C.C. Huang, J. Bai, R. Pindak, H.F. Gleeson, Europhys. Lett. **72**, 976 (2005).
18. The criterion taken here is that a satellite peak can be resolved if its distance from the non-resonant integer Bragg peak is at least twice the width of the peaks, *i.e.* $2\times 5\cdot 10^{-4}$ Å^{-1}.
19. J. Philip, J.-R. Lalanne, J.-P. Marcerou, G. Sigaud, Phys. Rev. E **52**, 1846 (1995).